Quantum geometry and the stability of fractional Chern insulators

Mathi Raja, Bartholomew Andrews, Michael Zaletel

Physics Department, UC Berkeley

Introduction

As the original example of a topological phase of matter with fractional excitations, the fractional quantum Hall effect has motivated significant research efforts, and the possible applications in quantum metrology and computing are exciting. Normally, fractional quantum Hall states require low temperature/high magnetic fields to be realized, however, in the two-dimensional lattice generalization known as fractional Chern insulators (FCIs), fractional quantum Hall states have the potential to be realized at zero magnetic field and at room temperature[1, 2, 3]. Furthermore, FCIs introduce more parameters to tune, such as the first Chern number leading to interesting novel phases. This makes FCIs especially appealing for applications like topological quantum computing, so in the past decade, significant theoretical interest has focused on FCIs [4].

Throughout the literature, the stability of FCIs has been shown to be related to the resemblance to Landau Levels, depending on band flatness, Berry curvature, and more recently the Fubini-Study (FS) metric is also shown to play a role in determining their stability [5]. To investigate this further, we focus on the zero-quadratic model (ZQM), as this model has been found to be able to specifically tune certain measures of FCI stability without affecting other quantities related to band geometry.

Single-particle Spectrum

Motivated as an extension of the Harper-Hofstadter (HH) model, we introduce a 3rd nearest-neighbor hopping to arrive at the zero-quadratic model (ZQM) [6]:

$$H = t_1 \sum_{ij_1} e^{i\theta_{ij}} c_i^\dagger c_j + t_3 \sum_{ij_3} e^{i\theta_{ij}} c_i^\dagger c_j + V \sum_{ij_1} \rho_i \rho_j + \text{H.c.} \tag{1}$$

Diagonalizing this Hamiltonian, we get the following example band structure at $t_3 = -\frac{1}{4}$ and $n_\phi = \frac{1}{5}$. The Chern numbers for each respective band are shown to the left of the plot and the magnetic Brillouin zone (ranging from 0 to $2\pi/5$ in the k_x direction and from 0 to 2π in the k_y direction) is discretized by 100 in each direction.

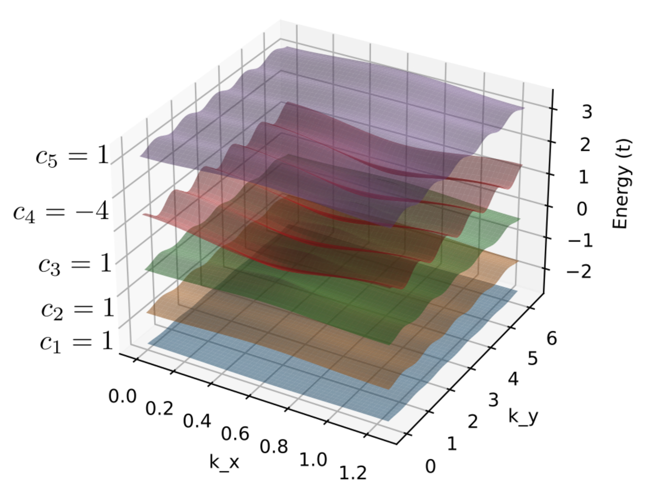

To understand the topological nature of our bands, we must compute the necessary topological invariant: Chern numbers (as motivated by the TKNN formula showing the Hall conductivity of a system is a topological invariant) [7]. Although the first Chern number is defined as the integration of the Berry curvature over the Brillouin Zone, we can use the Fukui formula to compute it efficiently [8]:

$$c_n = \frac{1}{2\pi} \sum_{\mathbf{k}\in \mathrm{BZ}} \operatorname{Im} \ln \left[U^{(n)}_{\mathbf{k}_1 \to \mathbf{k}_2} U^{(n)}_{\mathbf{k}_2 \to \mathbf{k}_3} U^{(n)}_{\mathbf{k}_3 \to \mathbf{k}_4} U^{(n)}_{\mathbf{k}_4 \to \mathbf{k}_1} \right] \tag{2}$$

with $U^{(n)}_{\mathbf{k}_\alpha \to \mathbf{k}_\beta} \equiv \frac{\langle \mathbf{u}_{n,e,\mathbf{k}_\alpha} | \mathbf{u}_{n,e,\mathbf{k}_\beta} \rangle}{\left| \langle \mathbf{u}_{n,e,\mathbf{k}_\alpha} | \mathbf{u}_{n,e,\mathbf{k}_\beta} \rangle \right|}$ known as link variables [8].

To further showcase the topological nature of the Chern number, we can also plot the Wilson loops, the product of Berry phases along a periodic loop in one direction along the Brillouin Zone as seen in Fig. 1 and Fig. 2:

The Wilson loops have a winding number around the Brillouin Zone identical to the magnitude of the respective band's Chern number and the sign of the Chern number describes its orientation. For our band structure, a band with Chern number 1 creates a Wilson loop along k_x of winding number 1 while for a band with Chern number -4, a Wilson loop of winding number 4 and flipped orientation.

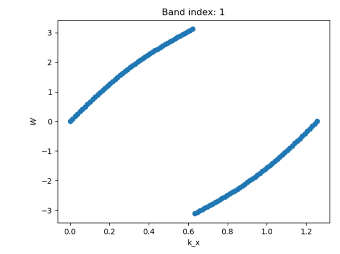

Figure 1. Wilson loop for $c_1 = 1$ band

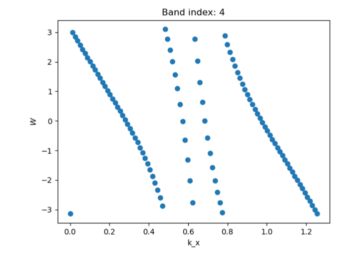

Figure 2. Wilson loop for $c_4 = -4$ band

Quantum Geometry

We introduce band geometry through the quantum geometric tensor (QGT) given as [9, 10]:

$$\mathcal{R}^s_{ab} = [\partial_{k_a} u^s(k)] \mathcal{Q}^s(k) [\partial_b u^s(k)] \tag{3}$$

where $\mathcal{Q}^s(k) = 1 - \sum_{r\neq s} k^r k^r$. Intuitively, the QGT can be thought of as a distance of Bloch eigenvectors on a Bloch sphere. The QGT can further be broken into its real and imaginary components represented by the Fubini-Study (FS) metric (g^s_{ab})and the Berry curvature (Ω^s_{ab}) respectively:

$$\mathrm{Re}(\mathcal{R}^s_{ab}) = g^s_{ab} = \frac{1}{2}(\langle \partial_{k_a} u^s(k) | \partial_{k_b} u^s(k) \rangle - \langle \partial_{k_a} u^s(k) | u^s(k) \rangle \langle u^s(k) | \partial_{k_b} u^s(k) \rangle + a \leftrightarrow$$

$$-2\mathrm{Im}(\mathcal{R}^s_{ab}) = \Omega^s_{ab} = i(\langle \partial_{k_a} u^s(k) | \partial_{k_b} u^s(k) \rangle - \langle \partial_{k_b} u^s(k) | \partial_{k_a} u^s(k) \rangle \tag{5}$$

It is further shown that these two inequalities based on the quantum geometric tensor must be satisfied [6, 11, 5]:

$$\mathrm{Det} g(k) \geq \frac{1}{4} |\mathcal{B}(k)|^2, \quad \mathrm{Tr} g(k) \geq |\mathcal{B}(k)|, \tag{6}$$

where $\mathcal{B}(k)$ is the Berry curvature.

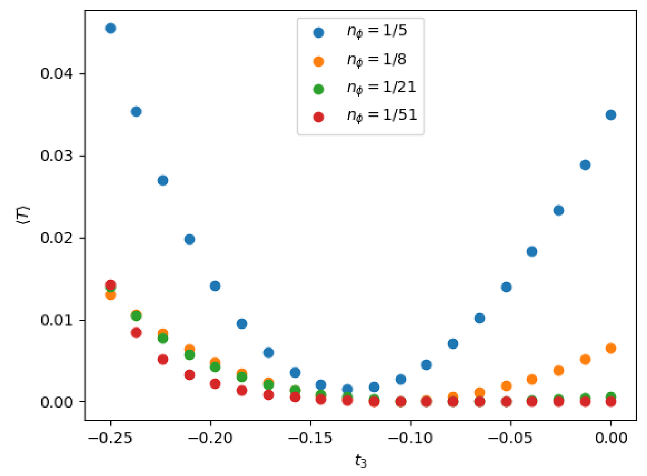

Figure 3. Plot showing the integrated TISM being satisfied as n_ϕ becomes smaller. Data is taken at various $n_\phi = 1/q$ values. The line at $t_3 = -0.25$ corresponds to the zero-quadratic point and $t_3 = 0$ corresponds to the Hofstadter model.

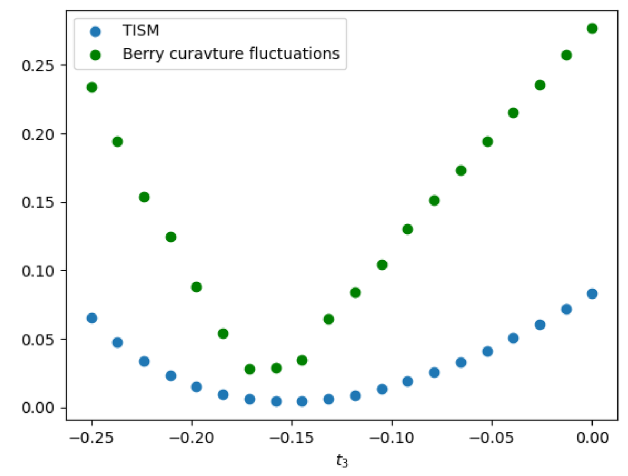

Figure 4. Plot showing the relationship between fluctuations of the Berry curvature and $\langle \mathcal{T} \rangle$ when varying t_3.

Many-Body Spectrum

To include many-body effects, we must now introduce a non-zero interaction strength, V, and consider interaction behavior. To start, we restrict interactions to a nearest-neighbor density-density interaction potential for fermions and on-site contact interaction for bosons. To numerically simulate the interaction, we use an infinity density matrix renormalization group algorithm (iDMRG) implemented via TeNPy [12, 13].

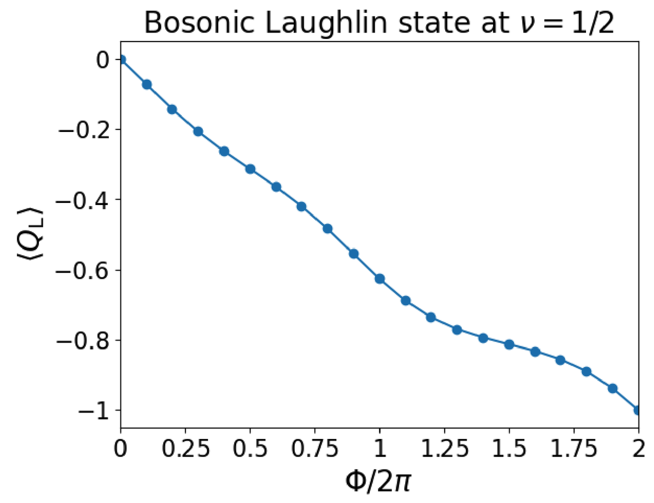

Figure 5. Charge pumping for the bosonic Laughlin state in the lowest band of the ZQM.

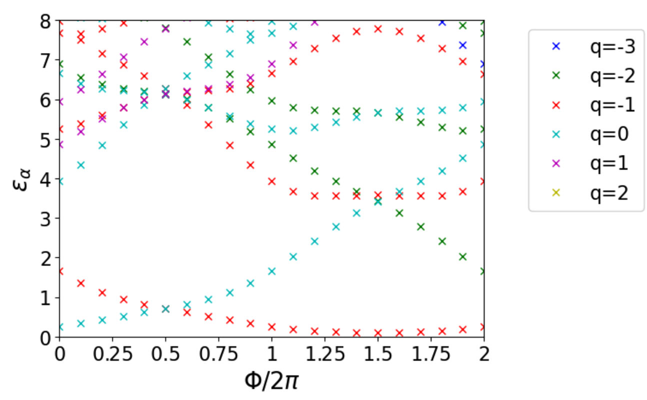

Figure 6. Spectral flow for the bosonic Laughlin state in the lowest band of the ZQM.

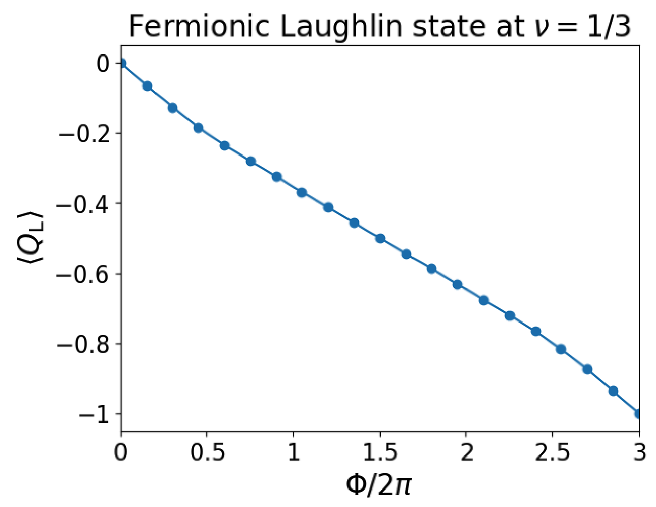

Figure 7. Charge pumping for the fermionic Laughlin state in the lowest band of the ZQM.

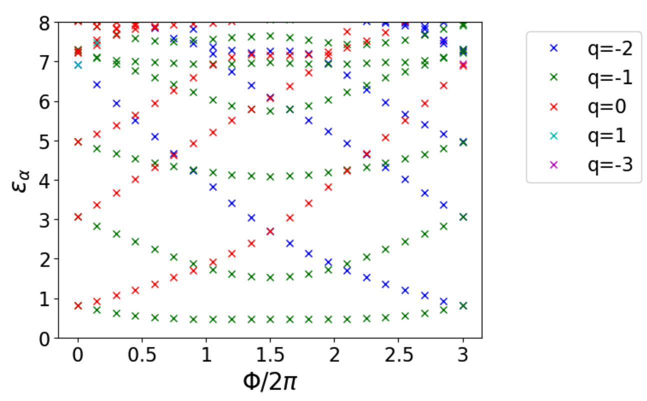

Figure 8. Spectral flow for the fermionic Laughlin state in the lowest band of the ZQM.

References

[1] Bartholomew Andrews, Titus Neupert, and Gunnar Möller. Stability, phase transitions, and numerical breakdown of fractional chern insulators in higher chern bands of the hofstadter model. *Phys. Rev. B*, 104:125107, Sep 2021.

[2] Titus Neupert, Luiz Santos, Claudio Chamon, and Christopher Mudry. Fractional quantum Hall states at zero magnetic field. *Phys. Rev. Lett.*, 106:236804, Jun 2011.

[3] Evelyn Tang, Jia-Wei Mei, and Xiao-Gang Wen. High-temperature fractional quantum Hall states. *Phys. Rev. Lett.*, 106:236802, Jun 2011.

[4] Emil J. Bergholtz and Zhao Liu. Topological flat band models and fractional chern insulators. *International Journal of Modern Physics B*, 27(24):1330017, 2013.

[5] T. S. Jackson, Gunnar Möller, and Rahul Roy. Geometric stability of topological lattice phases. *Nature Communications*, 6(1):8629, November 2015.

[6] David Bauer, Spenser Talkington, Fenner Harper, Bartholomew Andrews, and Rahul Roy. Fractional Chern insulators with a non-Landau level continuum limit. *Phys. Rev. B*, 105:045144, Jan 2022.

[7] Qian Niu, D. J. Thouless, and Yong-Shi Wu. Quantized hall conductance as a topological invariant. *Phys. Rev. B*, 31:3372–3377, Mar 1985.

[8] Takahiro Fukui, Yasuhiro Hatsugai, and Hiroshi Suzuki. Chern numbers in discretized brillouin zone: Efficient method of computing (spin) hall conductances. *Journal of the Physical Society of Japan*, 74(6):1674–1677, 2005.

[9] Ran Cheng. Quantum geometric tensor (fubini-study metric) in simple quantum system: A pedagogical introduction. 12 2010.

[10] David Bauer, T. S. Jackson, and Rahul Roy. Quantum geometry and stability of the fractional quantum hall effect in the hofstadter model. *Phys. Rev. B*, 93:235133, Jun 2016.

[11] Rahul Roy. Band geometry of fractional topological insulators. *Phys. Rev. B*, 90:165139, Oct 2014.

[12] Johannes Hauschild and Frank Pollmann. Efficient numerical simulations with Tensor Networks: Tensor Network Python (TeNPy). *SciPost Phys. Lect. Notes*, page 5, 2018. Code available from `https://github.com/tenpy/tenpy`.

[13] Adolfo G. Grushin, Johannes Motruk, Michael P. Zaletel, and Frank Pollmann. Characterization and stability of a fermionic $\nu = 1/3$ fractional chern insulator. *Phys. Rev. B*, 91:035136, Jan 2015.

mathiraja@berkeley.edu